# Periodic DFT Study of the Pt(111): A p(1×1) Atomic Oxygen Interaction with the Surface

**Anton Kokalj,*,† Antonija Lesar,† Milan Hodošček,†,‡ and Mauro Causà§**

*Department of Physical and Organic Chemistry, J. Stefan Institute, Jamova 39, SI-1000 Ljubljana, Slovenia, and Department of Inorganic, Physical and Materials Chemistry, University of Torino, Via P. Giuria 5, I-10125 Torino, Italy*

*Received: March 5, 1999; In Final Form: June 2, 1999*

The p(1×1) adsorption of atomic oxygen on the fcc and hcp three-fold hollow site of a Pt(111) surface has been investigated by a periodic slab model, varying the number of layers from two to four. The density functional method with local spin density approximation and with generalized gradient exchange−correlation functionals was employed using the CRYSTAL95 ab initio program. It was found that the three-layer slab model was a good compromise between accuracy and the computational time. The LDA/VWN calculations predict that the fcc-hollow site is energetically preferable by 0.29 eV compared to the hcp-hollow site. This preference is also supported by experimental data. Oxygen p(1×1) heat of adsorption of 0.61 eV calculated with the BPW91 method is in reasonable agreement with the experimentally estimated one. The corresponding equilibrium adsorbate−surface distance is 1.25 Å. Density-of-states analysis demonstrates that the formation of the Pt−O bond is mainly due to the interaction of Pt $5d_{xz}$ and $5d_{yz}$ orbitals of the surface platinum atom and $2p_x$ and $2p_y$ orbitals of the oxygen adatom. Three-dimensional difference electron density plots indicate a delocalized interaction of the oxygen adatoms to the surface.

## Introduction

Platinum surfaces are of a wide scientific and technological interest, particularly because of their catalytic properties in the oxidation of carbon monoxide.[1,2] The mechanism of this surface reaction involves few elementary steps; oxygen chemisorption is essential to understanding the catalytic process. Namely, the oxidation of CO on platinum metals is likely to take place on oxygen adsorption sites[3] since the mobility of CO is much higher than the mobility of the oxygen adatoms.[4]

A variety of experimental surface science techniques have been employed to investigate the adsorption of the oxygen on Pt(111).[5−11] Most authors agree that the saturation coverage of the oxygen adsorption on this surface is about 0.25 monolayer (ML) and forms the p(2×2) structure, with the O atom bound in the fcc three-fold hollow position. There is some disagreement about the oxygen height above the surface. Mortensen et al.[10] reported the height at 0.85 Å, whereas Starke et al.[12] estimated it to be 1.18 Å. A recent study by Materer et al.[13] provided the oxygen height of 1.19 Å. Heats of oxygen adsorption ranging from 2.16 to 5.20 eV at low oxygen coverage have been reported.[6−8,14] Estimates for the heat of adsorption at high coverage corresponding to the p(2×2) structure are more consistent. Gland et al.[7] determined the high coverage heat of adsorption to be about 1.65 eV. Yeo et al.[14] obtained practically the same value, whereas Campbell et al.[8] and Parker et al.[15] reported the energies of 1.82 and 1.86 eV, respectively. On the other hand, a still higher coverage can be achieved by the stimulated dissociation of the molecularly adsorbed $O_2$[16] or by the decomposition of the adsorbed $NO_2$.[15] This higher coverage state can also be formed by the adsorption of $O_2$ at high temperature (540 K) and high oxygen pressure ($10^{-3}$ Pa).[17] Under similar surface conditions Neuhaus et al.[18] found the p(1×1) structure for the atomic oxygen overlayer by He scattering measurements. It should be mentioned that the XPS characterization[17] of this adsorbate phase showed the same chemical state of the oxygen as for the adsorption at lower coverage. This was also confirmed by Parker et al.[15] using various spectroscopic methods.

Theoretical investigations concerning the oxygen adsorption on the platinum surface were scarce until some years ago. Calculations using a cluster model[19−23] as well as a periodical approach[24−31] are available in the literature. An earlier molecular orbital study was performed by Ray and Anderson[20] using an atom superposition and electron delocalization technique. These calculations proposed the binding energy of 3.01 eV for the oxygen on a three-fold site on the $Pt_4$ model of Pt(111). Recent cluster calculations for the $O_2$/Pt(111) system by Kokalj et al.[23] confirms the dissociative oxygen adsorption on $Pt_3$ and $Pt_4$ surface models. The interaction energies of 3.99 and 3.56 eV for Møller−Plesset second order perturbation and generalized gradient calculations, respectively, on the $Pt_3$ surface model were obtained. The corresponding surface−oxygen distances are 1.1 and 1.2 Å, respectively. Illas et al.[22] reported a systematic study of correlated effects on adsorption properties using the one-electron approximation and analyzed the bonding of oxygen on $Pt_9$ and $Pt_{25}$ cluster models of the Pt(111) surface. They showed that the bonding of oxygen to platinum has a partial ionic character and that the effect of correlation is to enhance the importance of covalent contributions to the bonding. Eichler et al.[28] studied molecular precursors in the dissociative adsorption of $O_2$ on Pt(111) by ab initio periodic local spin density calculations. The heat of adsorption of the atomically adsorbed oxygen was calculated to be 1.65 eV for the fcc-hollow position. Feibelman's[27] local density functional calculations for p(2×2)O/Pt(111) predict that O adatoms favor fcc over hcp positions by roughly 0.5 eV. The structural-energy difference is explained

† Department of Physical and Organic Chemistry.
‡ Also at the Center for Molecular Modeling, National Institute of Chemistry, Hajdrihova 19, SI-1000 Ljubljana, Slovenia.
§ Department of Inorganic, Physical and Materials Chemistry.

10.1021/jp990788b CCC: $18.00 
Published on Web 08/07/1999

by d-electron depletion between first- and second-neighbor Pt atoms in the fcc binding geometry. Bogicevic et al.[29] investigated the diffusion barrier for the atomic oxygen on Pt(111) using first-principle periodic density functional methods. Their calculated surface relaxation and the buckling of the surface atoms are in good agreement with the experimental data provided by Starke et al.[12] and Materer et al.[13] Binding energies of the fcc-hollow site were calculated to be 5.18 eV by the local spin density approximation, and 4.23 eV by the generalized gradient approximation, whereas the diffusion barrier from the fcc to hcp site was 0.58 eV. Recent theoretical work of CO oxidation on Pt(111) showed that O adatoms bonded on the hollow sites are approximately 0.6 eV more stable than the structures with O atoms on bridge sites.[30]

So far, no theoretical study concerning p(1×1) O adsorption on Pt(111) surface has been reported in the literature. The availability of experimental data for that high coverage phase allows the comparison of the experimental data with the results from first-principle methods. The aim of this paper is to present detailed theoretical investigation of the atomic oxygen adsorption on the platinum surface at full coverage ($\theta = 1$, one O atom per one surface Pt atom) performed with the LCAO periodic density functional method. We will focus on the calculation of adsorption energetics on fcc and hcp three-fold hollow sites on the (111) surface. The electronic structures will be examined with emphasis on chemical bonding of oxygen adatoms with the surface. The origin of fcc vs hcp binding preference will be discussed.

## Computational Method

The calculations were performed using the CRYSTAL95 program.[33] Linear combinations of Gaussian-type orbitals were used as variational functions. Since all-electron basis-sets are not practical from a computational viewpoint, the relativistic effective-core potential (RECP) was used to describe the inner shells of Pt atoms. The RECP of Stevens et al.[34] was taken, and the *f*-projection term was omitted since our previous cluster calculations showed that the influence of *f*-projection term is negligible.[35] For Pt valence electrons the basis set of the same authors contains two very diffuse functions; therefore, it had to be modified. Except for one diffuse d-shell and one diffuse sp-shell, the most diffuse sp and d functions were omitted, because in periodic systems such functions can lead into wasting of computational resources or even cause a basis set linear dependency. Thus, instead of the original basis set expressed in the terms of (7s7p5d/4s4p3d), the (6s6p4d/3s3p2d) basis set was used. The basis set produced in this way is of double-zeta quality. Oxygen atoms were described by the 6-311G* basis set,[36] which contains a polarization d-shell. The presence of a polarization shell can ensure a possible charge transfer from substrate to the adsorbate. The calculations were performed using the local spin density approximation. The exchange potential of Dirac−Slater[37] (LDA) and the correlation potential of Vosko−Wilk−Nusair[38] (VWN) were used. Heat of adsorption was also estimated by using nonlocal gradient corrections with the exchange potential of Becke[39] and correlation potential of Perdew−Wang[40] (BPW91).

Theoretical description of metallic systems is more critical than those of ionic or covalent systems since very delocalized bands are described poorly by the LCAO. However, some metal systems have been studied by this method.[25−27,41−44] A self-consistent-field (SCF) convergence is very poor, especially when some symmetry is broken, as is in the case of slabs. Methods dealing with an acceleration of the SCF convergence are of great importance. We found that a very simple two-point mixing of the Kohn−Sham matrixes with variable coefficients, as described by Morruzi−Janak−Wiliams[45] for mixing the densities, coupled with the Pulay's DIIS extrapolation (direct-inversion of iterative subspace)[46] can help appreciably. The best results are accomplished by applying the two-point mixing as well as DIIS extrapolation when the energy convergence is lower than $10^{-2}$ au. Unrestricted calculations improve convergence problems significantly even in the singlet case ($S = 0$). Because of the additional variational freedom the unrestricted energy should lie, in principle, below the restricted one, but the difference is negligible as long as the system is near equilibrium geometry. Nineteen-k points of a Monkhorts net[47] in the irreducible part of the Brillouin zone were used for slab calculations. Bands were interpolated by 87 symmetrized plane waves in denser nets (Gilat net[48]) of 61-k points. Fermi surface was then approximated quadratically in a spherical domain around each k-point of the Gilat net.

The surface was modeled by periodic slabs, the number of layers varying from two to four. For the Pt−Pt bond distance, the bulk bond distance of 2.772 Å from LDA/VWN calculations[32] was taken. This distance corresponds to the lattice constant of 3.92 Å and coincides with the experimental value.[49] The atomic oxygen overlayer in the p(1×1) periodicity was adsorbed on both sides of the slab. Thus our model requires just one atom per layer. Two settings of the adsorbed oxygen were considered, one on the fcc-hollow, and one on the hcp-hollow position, as shown in Figure 1. Individual atoms will be denoted as $Pt_{(1)}$ for the surface platinum atom, $Pt_{(2)}$ for the subsurface platinum atom, and $O_{(1)}$ for the oxygen adatom.

Interaction energy curves of the oxygen monolayer with the platinum surface were obtained by the rigid displacement of the adsorbate monolayer from the surface and evaluated according to the expression:

$$\Delta E(d) = \frac{E_{\mathrm{O/SX}}(d) - (E_{\mathrm{SX}} + 2E_{\mathrm{O_{ML}}})}{2}, \quad X = 2, 3, \text{ and } 4 \qquad (1)$$

where $E_{\mathrm{O/SX}}(d)$ is the total energy of the adsorbate/substrate system at an adsorbate−surface distance $d$, $E_{SX}$ is the total energy of the bare Pt(111) slab, $E_{\mathrm{O_{ML}}}$ is the total energy of the p(1×1) oxygen monolayer, and X labels the number of layers in the slab model.

The binding energy between the single oxygen atom and the platinum surface $E_{\mathrm{O-Pt_{surf}}}$ can be approximated by

$$E_{\mathrm{O-Pt_{surf}}} = -\frac{E_{\mathrm{O/SX}}(d_0) - (E_{SX} + 2E_{\mathrm{O}})}{2}, \quad X = 2, 3, \text{ and } 4 \qquad (2)$$

where $E_{\mathrm{O/SX}}(d_0)$ corresponds to the total energy of the O/SX system at the equlibrium distance $d_0$ and $E_O$ is the total energy of the free oxygen atom.

As a first approximation, the heat of adsorption per $O_2$ was obtained from the relation[50]

$$\Delta H_{\mathrm{ads}} = -(E_{\mathrm{O/SX}}(d_0) - (E_{SX} + E_{\mathrm{O_2}})), \quad X = 2, 3, \text{ and } 4 \qquad (3)$$

where $E_{\mathrm{O_2}}$ corresponds to the total energy of the isolated oxygen molecule. This heat of adsorption corresponds to the process $O_{2(g)} \rightarrow 2O_{(ad)}$.[8]

## Results and Discussion

**Adsorption Energetics.** In our previous work (to be published elsewhere),[32] we investigated surface features of Pt(111)

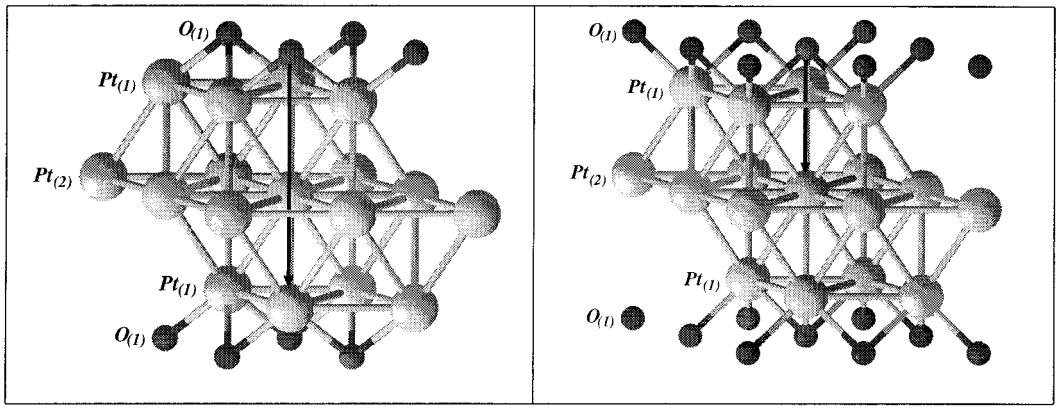


**Figure 1.** Three-layer slab used as a model of adsorption. Two unit cells in both crystallographic directions parallel to the (111) surface are shown. An oxygen monolayer in a p(1×1) periodicity is adsorbed on both sides of the slab. Individual atoms are denoted as $Pt_{(1)}$ for surface platinum atom, $Pt_{(2)}$ for subsurface platinum atom, and $O_{(1)}$ for oxygen adatom. Left: fcc-hollow position of oxygen adatoms. Right: hcp-hollow position of oxygen adatoms. Arrows indicate the position of oxygen with respect to subsurface layers. On the fcc-hollow position, oxygen adatoms coincide with the third platinum layer, whereas on the hcp-hollow position oxygen adatoms coincide with the second platinum layer. (These pictures were produced with the *XCrySDen* graphical package.[52])

slabs of different thickness. Some results can be summarized as follows: (i) the relaxation energies are of the order of $10^{-3}$ eV. Two- and four-layer slabs exhibit an outward relaxation of 0.01 Å, but for the three-layer slab an inward relaxation of −0.02 Å is found. Because of these small values, the slab relaxation could be ignored in modeling the Pt(111) surface. (ii) The quadrupole moment components perpendicular to the slab show an elongation of the surface atom's electron cloud for all slab models and a squeezing of the sublayer atom's electron cloud for the three and four-layer slabs. The picture of the quadrupole moment analysis is confirmed by the difference electron density plots. (iii) The band structures of the studied slab models are very similar and show a good correspondence to the (111) projected bulk band structure. (iv) The density-of-states is found as the most dependent property of the slab thickness. Density-of-states curves, difference electron density maps, and the Mulliken orbital population analysis demonstrate that the first sublayer is not yet an adequate bulk layer.

Here, we have examined the influence of the oxygen adatoms on the relaxation of the platinum surface layer. Figure 2 shows the relaxation energy curves for $O/S3_{fcc}$ and $O/S4_{fcc}$ slabs. The curves were evaluated by fixing the oxygen adatoms at the equilibrium adsorbate−surface distance obtained from calculations, where the relaxation was not considered. Then, the surface layer and oxygen monolayer were rigidly displaced. The relaxation distance of the surface platinum layer is −0.016 Å and −0.019 Å for $O/S3_{fcc}$ and $O/S4_{fcc}$, respectively. The relaxation energy is less than 0.01 eV in both cases. Thus these small relaxation distances and energies should be of minor importance; therefore, the relaxation was not taken into account for below oxygen binding energy calculations. Judging from the relaxed bare four-layer slab, the oxygen adatoms push the platinum surface layer toward the interior of the slab for about 0.03 Å. Relaxation for the bare four-layer slab is 0.01 Å outward.

When studying the interaction of the oxygen monolayer with the Pt(111) surface, possible spin multiplicities should be considered. The spin multiplicity of an atomic and molecular oxygen ground state is a triplet, i.e., the ground state is $^3P$ and $^3\Sigma_g^-$ for atomic and molecular oxygen,[51] respectively, whereas the spin multiplicity of the ground state for the Pt(111) slabs is a singlet.[32] The spin multiplicity of the isolated oxygen monolayer was investigated, and the triplet state was found to be the lowest in energy, lying 1.14 eV below the singlet state.

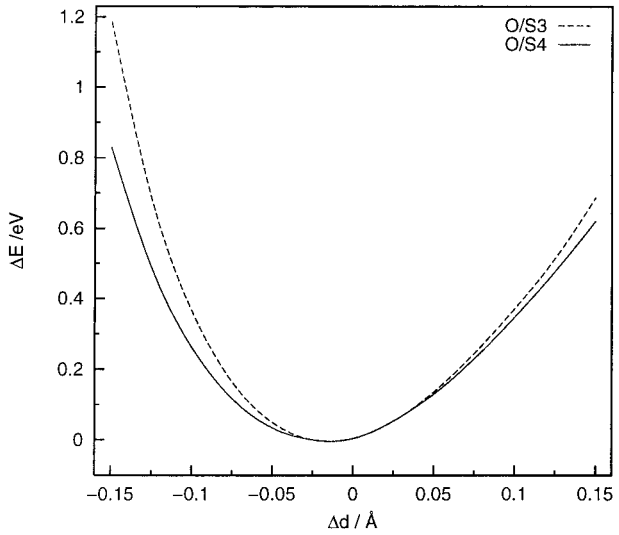


**Figure 2.** LDA/VWN relaxation energy curves for $O/S3_{fcc}$ and $O/S4_{fcc}$ slabs. They were obtained by fixing the oxygen adatoms at equilibrium adsorbate−surface distance evaluated from Figure 3, where the relaxation was not accounted for. Then the surface layer and the oxygen monolayer were rigidly displaced.

Hence, singlet, triplet, and pentet spin multiplicities were considered for the interaction between the slabs and oxygen overlayer. The interaction energy curves of the oxygen monolayer with the S2, S3, and S4 slabs as a function of the adsorbate−surface distance $d$ are presented in Figure 3. $O/SX_{fcc}$ and $O/SX_{hcp}$ denotations are related to fcc- and hcp-hollow position of oxygen, respectively, on the S$X$ slabs ($X$ = 2, 3, and 4). The zero energy corresponds to $E_{SX} + 2E_{O_{ML}}$, where $E_{O_{ML}}$ represents the total energy of the oxygen monolayer in the triplet state. In Table 1 equilibrium adsorbate−surface distances ($d_0$), and the binding energies of oxygen monolayer with surface ($E_b$) are summarized. Binding energy is related to the negative value of the interaction energy at equlibrium distance, i.e., $E_b = -\Delta E(d_0)$. It is evident that the singlet state gives the highest binding energies and shortest equilibrium distances. An exception is the O/S2 system where the singlet and triplet states are quite close, and the triplet state exceeds the singlet state in $O/S2_{hcp}$ case. It is also evident that the fcc-hollow position of the oxygen adatoms is preferred over the hcp-hollow position. Therefore, in the subsequent discussion only the singlet state and the fcc position of the oxygen adatoms

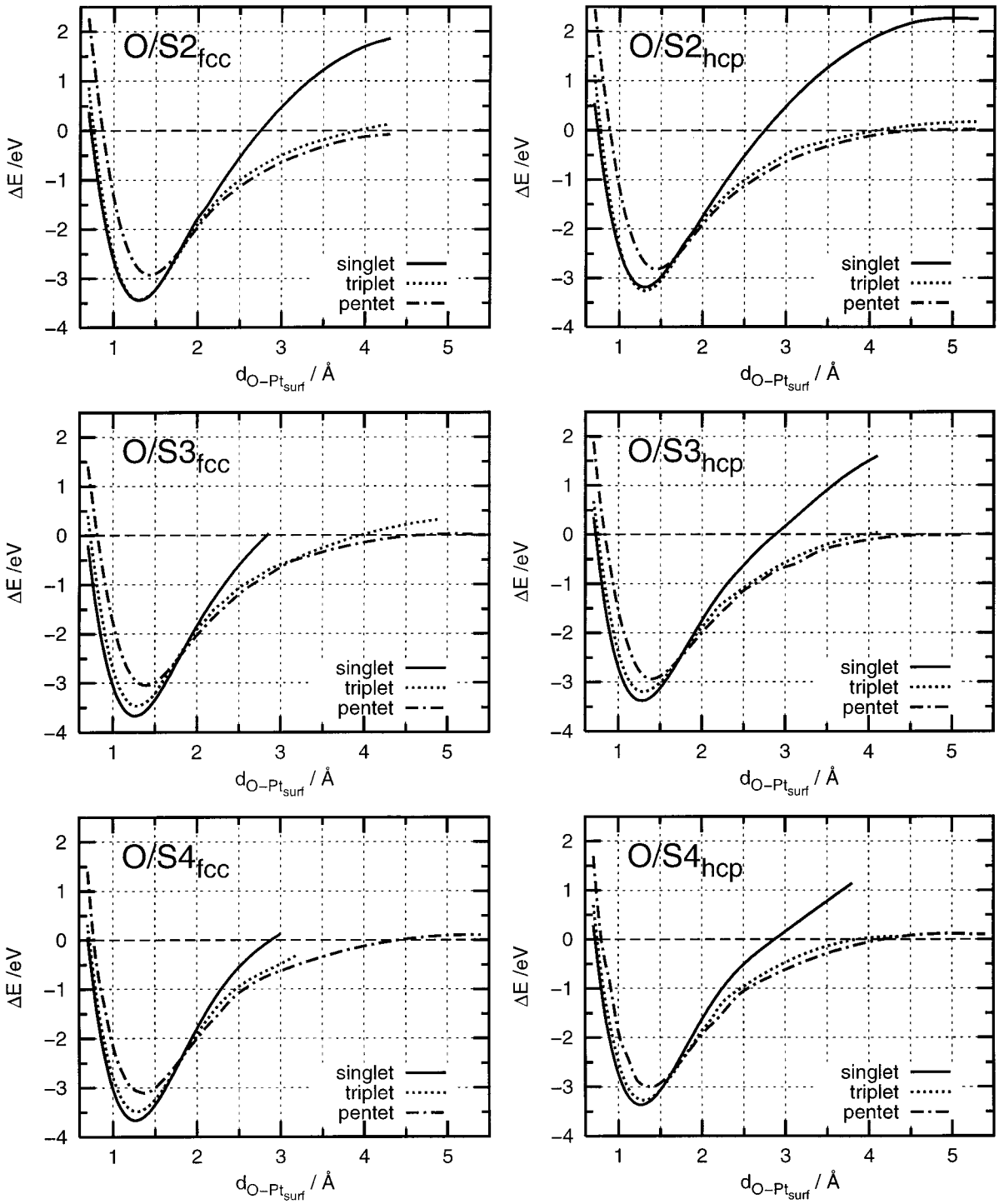


**Figure 3.** LDA/VWN interaction potentials of oxygen monolayer with platinum slabs. From top to bottom, potentials for O/S2, O/S3, and O/S4 systems are plotted. On the left parts, interaction potentials for the fcc-position are drawn, whereas on the right parts, potentials for the hcp-position are drawn. On each part, potentials for singlet, triplet, and pentet spin multiplicities are presented. The zero energy corresponds to $E_{SX} + 2E_{O_{ML}}$, where $E_{O_{ML}}$ represents the total energy of the oxygen monolayer in the triplet state.

will be concerned. From Figure 3 and Table 1, a good convergence of the interaction potentials with the increasing slab thickness can be inferred. Three- and four-layer slabs give practically equal binding energy and equilibrium adsorbate-surface distance, whereas the two-layer slab gives about 6% lower binding energy and about 3% larger equilibrium distance compared to the former. Equilibrium adsorbate−surface distance of the O/S3 and O/S4 is 1.265 Å and is comparable with the experimentally estimated value of 1.18 Å[12] and 1.19 Å.[13] It is worth noting that our distance corresponds to the p(1×1), whereas the experimentally obtained distance corresponds to the p(2×2) monolayer of the adsorbed oxygen adatoms. For the p(1×1) adsorption each surface platinum atom is bonded to three oxygen adatoms, but in the case of the p(2×2) adsorption only three out of four surface platinum atoms are bonded to the oxygen adatoms, where each bonded platinum atom is bonded exactly to one oxygen adatom (see refs 12 and 13 for graphical illustration). Consequently, the coordination number of the surface platinum atom is increased in the case of p(1×1) adsorption with respect to the p(2×2) adsorption. As pointed out by Parker et al.,[15] the greater coordination number is the reason for weakening the adsorbate/surface bond

**TABLE 1: LDA/VWN Equilibrium Adsorbate−Surface Distances $d_0$ and Binding Energies of the Oxygen Monolayer with Platinum Surface $E_b$[a]**

| | | singlet | | triplet | | pentet | |
|---|---|---|---|---|---|---|---|
| | site | $d_0$/Å | $E_b$/eV | $d_0$/Å | $E_b$/eV | $d_0$/Å | $E_b$/eV |
| O/S2 | fcc | 1.303 | 3.45 | 1.302 | 3.44 | 1.430 | 2.93 |
| | hcp | 1.304 | 3.19 | 1.308 | 3.26 | 1.448 | 2.82 |
| O/S3 | fcc | 1.265 | 3.67 | 1.287 | 3.47 | 1.394 | 3.05 |
| | hcp | 1.286 | 3.38 | 1.300 | 3.20 | 1.406 | 2.94 |
| O/S4 | fcc | 1.265 | 3.67 | 1.280 | 3.51 | 1.355 | 3.11 |
| | hcp | 1.270 | 3.37 | 1.295 | 3.28 | 1.375 | 3.00 |

[a] Two-, three-, and four-layers slabs and singlet, triplet, and pentet spin multiplicities are considered.

**TABLE 2: Binding Energies Corresponding to the Oxygen Monolayer $E_b$, the Oxygen Atom $E_{O-Pt_{surf}}$, and Heats of Adsorption $\Delta H_{ads}$, for O/S2$_{fcc}$, O/S3$_{fcc}$, and O/S4$_{fcc}$ Systems with Singlet Spin Multiplicity[a]**

| method | system | $E_b$/eV | $E_{O-Pt_{surf}}$/eV | $\Delta H_{ads}$/eV |
|---|---|---|---|---|
| LDA/VWN | O/S2$_{fcc}$ | 3.45 | 4.39 | 1.41 |
| | O/S3$_{fcc}$ | 3.67 | 4.61 | 1.85 |
| | O/S4$_{fcc}$ | 3.67 | 4.61 | 1.85 |
| BPW91 | O/S3$_{fcc}$ | 2.90 | 3.22 | 0.61 |

[a] Energies were obtained according to eqs 1−3.

and elongation of the adsorbate/surface bond length. On the basis of their findings, the elongation of about 0.08 Å obtained in our calculations could be explained.

The binding energies presented in Table 1 can not be directly compared to the experimental data. Thus, the adsorbate/surface binding energy $E_{O-Pt_{surf}}$ and the heat of adsorption $\Delta H_{ads}$ were computed applying eqs 2 and 3, respectively. $E_b$, $E_{O-Pt_{surf}}$, and $\Delta H_{ads}$ for O/S$X_{fcc}$ systems are given in Table 2. Results of self-consistent BPW91 calculations are also presented for the O/S3$_{fcc}$ system. These BPW91 results were obtained from calculations using the BPW91 lattice constant. The heat of adsorption obtained by LDA/VWN functional equals 1.85 eV, whereas BPW91 gives the heat of adsorption of 0.61 eV. The latter value corresponds to the atomic oxygen binding energy $E_{O-Pt_{surf}}$ of 3.22 eV and is close to our previous value of 3.56 eV obtained by the cluster calculation.[23] It is worth noting that the cluster calculation is appropriate for the low coverage situation, whereas present periodic calculation can suit the full coverage situation. Thus, the lower value of the periodic calculation is in accordance with the fact that the binding energy decreases with the increasing coverage. An experimental heat of adsorption was measured by Yeo et al.[14] up to coverage of 0.7 ML. Extrapolation of those data gives the adsorption heat of about 1.15 eV at full coverage ($\theta = 1$), but Parker et al.[15] estimated the heat of adsorption to be less than 0.5 eV for the coverages $\geq$ 0.75 ML. From Table 1 it is clear that the fcc-hollow site is preferred over the hcp-hollow site, the difference being $\Delta E_{fcc/hcp} = 0.29$ eV, which is lower than those of 0.50 and 0.45 eV calculated by Feibelman[27] and by Bogicevic et al.,[29] respectively, for p(2×2) adsorption.

**Electronic Structures.** Before discussing electronic structures it is worth noting that several atomic orbitals are related among themselves due to a symmetry of O/S$X$ ($X$ = 2, 3, and 4) systems. Such related orbitals are $p_x$ vs $p_y$, $d_{xz}$ vs $d_{yz}$, and $d_{x^2-y^2}$ vs $d_{xy}$. For each pair the individual orbitals share the same orbital population, density of states curve, etc.

Table 3 presents a multipole analysis of the individual atoms up to the quadrupole. At the adsorbate−surface equilibrium distance the net charge transfer from substrate to oxygen is 0.32, 0.31, and 0.31 electrons for the O/S2$_{fcc}$, O/S3$_{fcc}$, and O/S4$_{fcc}$,

**TABLE 3: LDA/VWN Multipole Analysis in au of Bare and fcc-Oxygen-Adsorbed Platinum Slabs (Singlet Spin Multiplicity Is Taken for All O/S$X_{fcc}$ Slabs)[a]**

| | | S2 | S3 | S4 | O/S2$_{fcc}$ | O/S3$_{fcc}$ | O/S4$_{fcc}$ |
|---|---|---|---|---|---|---|---|
| $q$ | $Pt_{(1)}$ | 0.000 | −0.050 | −0.042 | −0.317 | −0.318 | −0.350 |
| | $Pt_{(2)}$ | | 0.100 | 0.042 | | 0.016 | 0.037 |
| | $O_{(1)}$ | | | | 0.317 | 0.310 | 0.313 |
| $D_z$ | $Pt_{(1)}$ | −288 | 2 | −117 | −656 | −633 | −575 |
| | $Pt_{(2)}$ | | 0 | 194 | | 0 | 40 |
| | $O_{(1)}$ | | | | 10 | −3 | −9 |
| $Q_z$ | $Pt_{(1)}$ | −1074 | −1279 | −1210 | 572 | 740 | 593 |
| | $Pt_{(2)}$ | | 241 | 103 | | −184 | −64 |
| | $O_{(1)}$ | | | | −94 | −3 | −6 |

[a] $D_z$ and $Q_z$ belong to a component perpendicular to the slab ($Q_z$ is a $2z^2 - x^2 - y^2$ component of the quadrupole moment).

respectively. Negative dipole moment values of the surface platinum atom for the O/S2$_{fcc}$, O/S3$_{fcc}$, and O/S4$_{fcc}$ along the direction perpendicular to the surface indicate a displacement of the electron cloud towards the oxygen adatom, whereas positive values of the quadrupole moment component perpendicular to the surface show a compression of the electron cloud around the surface platinum atoms. The subsurface atoms undergo the opposite change, that is, an expansion of their electron cloud. Very small values of the dipole and quadrupole moments for the oxygen adatom indicate that its electron cloud is sphere-like and centered near the nucleus. This picture is confirmed by the 3D difference electron density plots,[52] shown in Figure 4. The difference between the electron density of the O/S4$_{fcc}$ system, and a superposition of atomic densities is drawn at the differences of −0.02, 0.00, and +0.02 au. It is evident that the electron cloud of the oxygen atom is spherical, indicating that the adsorbate/surface bond is delocalized, although the difference density of the surface platinum atom indicates some localization. The delocalization is consistent with the fact that the O/S$X$ ($X$ = 2, 3, and 4) systems are metals, because a very localized adsorbate/surface bond could destroy the metallic character of the slabs. The electron charge transfer from the surface to adatoms is obvious. The subsurface layer participate in the electron charge transfer as well. The isosurface of zero value confirms the results of the quadrupole moment analysis; namely, the electron cloud of the surface platinum layer is compressed along the $z$-direction.

As shown in our previous work,[32] the surface atoms exhibit a redistribution of charge among and within s, p, and d shells. Mulliken population analysis can be applied to explore the influence of the oxygen adatom on the redistribution of charge. Results of Mulliken population analysis should be taken with care, since the analysis is basis set dependent. However, it can give some qualitative insight into bonding, particularly when similar systems calculated with the same basis set are compared. Moreover, the basis set employed here is not very diffuse, since the smallest Gaussian exponent is larger than 0.1 bohr$^{-2}$. Results of the shell and orbital population analysis for the O/S4$_{fcc}$ system with the equilibrium adsorbate−surface distance is presented in Table 4. The population of the O/S4$_{fcc}$ system is compared to the bare S4 slab and isolated oxygen monolayer $O_{ML}$ as well. Therefore, the difference between the O/S4$_{fcc}$ and S4 for the platinum atoms and between the O/S4$_{fcc}$ and $O_{ML}$ for the oxygen atom is reported in parentheses, which is designated as $\Delta_{a,b}$ ($a$ stands for the adsorbate/substrate system and $b$ for either the bare platinum slab, or for the isolated oxygen monolayer). The surface platinum atom population of the O/S4$_{fcc}$ is changed considerably, which is due to the presence of the adatoms. The net population of the d shell reveals a significant decrease in its occupation (−0.195 electrons), accompanied with the change

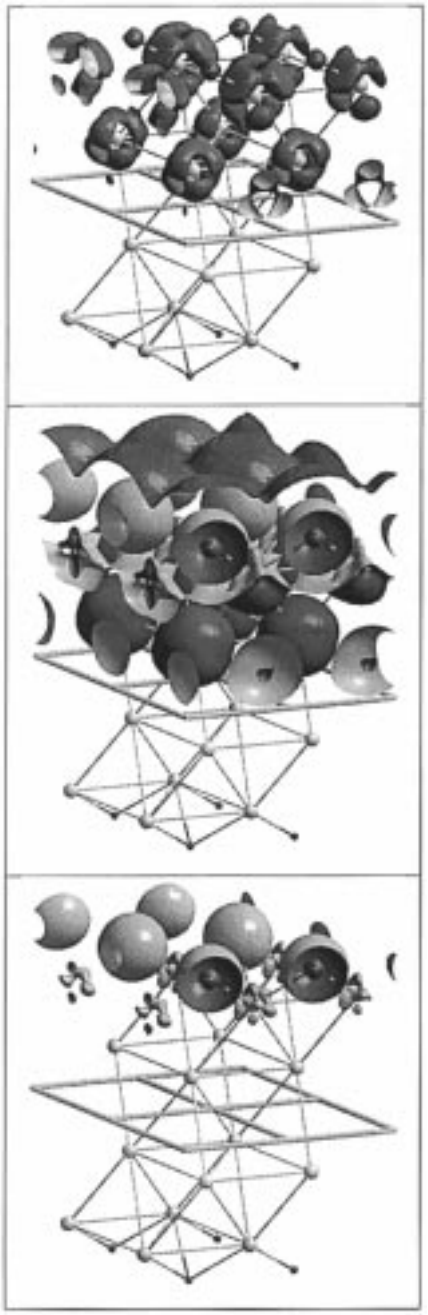

**Figure 4.** LDA/VWN difference electron density for the O/S4$_{fcc}$ system at the equilibrium adsorbate−surface distance. Difference electron density was obtained by subtracting a O/S4$_{fcc}$ density from a superposition of individual atomic densities, i.e., $\rho$(O/S4$_{fcc}$) − [$\rho$(Pt$_{atoms}$) + $\rho$(O$_{atoms}$)]. Two unit cells in both crystallographic directions parallel to the (111) surface are drawn as indicated by unit cell borders in the middle of slabs. Difference electron densities are cut along the outborders. From top to bottom, differences of −0.02, 0.00, and 0.02 au are drawn, respectively. (These pictures were produced with the *XCrySDen* graphical package.[52])

in population of the 5d$_{xz}$ and 5d$_{yz}$ orbitals. This indicates that the electron cloud around the Pt$_{(1)}$ atom might be compressed along the *z*-direction and is consistent with the 3D difference electron density maps and with the analysis of the quadrupole moments. There is also a charge transfer from the 6s, 6p$_x$, and 6p$_y$ orbitals of the Pt$_{(1)}$ atom (−0.163 electrons) to the oxygen adatoms. The charge from the substrate is transferred to the 2p$_x$ and 2p$_y$ orbitals of the oxygen.

Overlap population (OP) analysis between individual atoms is presented in Table 5. There is a good convergence of the

**TABLE 4: LDA/VWN Mulliken Population Analysis in au of O/S4$_{fcc}$ System in Singlet State at Equilibrium Adsorbate−Surface Distance[a]**

| | Pt$_{(1)}$ | Pt$_{(2)}$ | O$_{(1)}$ |
|---|---|---|---|
| 5sp ($\Delta_{a,b}$) | 8.028 (+0.049) | 8.028 (+0.001) | |
| 5d ($\Delta_{a,b}$) | 8.234 (−0.195) | 8.405 (+0.012) | |
| 6sp ($\Delta_{a,b}$) | 1.388 (−0.163) | 1.603 (−0.018) | |
| 5d$_{z^2}$ ($\Delta_{a,b}$) | 1.802 (+0.068) | 1.676 (−0.044) | |
| 5d$_{xz}$, 5d$_{yz}$ ($\Delta_{a,b}$) | 1.488 (−0.178) | 1.666 (+0.017) | |
| 5d$_{x^2-y^2}$ ($\Delta_{a,b}$) | 1.728 (+0.047) | 1.699 (+0.011) | |
| 6s ($\Delta_{a,b}$) | 0.626 (−0.126) | 0.722 (−0.004) | |
| 6p$_x$, 6p$_y$ ($\Delta_{a,b}$) | 0.253 (−0.039) | 0.293 (−0.001) | |
| 6p$_z$ ($\Delta_{a,b}$) | 0.256 (+0.040) | 0.295 (−0.013) | |
| 2p$_x$, p$_y$ ($\Delta_{a,b}$) | | | 1.419 (+0.157) |
| 2p$_z$ ($\Delta_{a,b}$) | | | 1.472 (+0.000) |
| 3d$_{z^2}$ ($\Delta_{a,b}$) | | | 0.002 (+0.002) |
| 3d$_{xz}$, 3d$_{yz}$ ($\Delta_{a,b}$) | | | 0.003 (+0.003) |
| 3d$_{x^2-y^2}$ ($\Delta_{a,b}$) | | | 0.001 (+0.001) |

[a] Shell and orbital populations for constituent atoms are presented. In parentheses the population difference with respect to bare S4 slab and isolated oxygen monolayer is reported for Pt and O atoms, respectively, designated as $\Delta_{a,b}$, where "a" stands for adsorbate−substrate system and "b" either for bare platinum slab or for free oxygen monolayer.

**TABLE 5: LDA/VWN Mulliken Overlap Population (OP) in au of Bonds between Constituent Atoms for Bare Slabs and Corresponding O/S*X*$_{fcc}$ Systems in Singlet State at Equilibrium Adsorbate−Surface Distance**

| bond | S2 | S3 | S4 | O/S2 | O/S3 | O/S4 |
|---|---|---|---|---|---|---|
| O−O | | | | −0.005 | −0.003 | −0.003 |
| O−Pt$_{(1)}$ | | | | 0.076 | 0.082 | 0.080 |
| Pt$_{(1)}$−Pt$_{(1)}$ | 0.152 | 0.155 | 0.154 | 0.063 | 0.061 | 0.060 |
| Pt$_{(1)}$−Pt$_{(2)}$ | | 0.110 | 0.113 | | 0.116 | 0.116 |
| Pt$_{(2)}$−Pt$_{(2)}$ | | 0.110 | 0.118 | | 0.119 | 0.119 |

OP's results for the increasing slab thickness. The negative values of the OP between oxygen adatoms indicate their repulsive attraction. Comparison of the OP between surface platinum atoms of the O/S*X*$_{fcc}$ systems and of the S*X* (*X* = 2, 3, and 4) slabs reveals a significant decrease in the OP between the surface platinum atoms. This may be explained by two facts: (1) the surface platinum atom of the O/SX$_{fcc}$ system has an increased coordination number (which reduces the OP) being equal to the coordination number of the bulk atom since adatoms form the p(1×1) pattern and (2) the charge transfer of 0.3 electrons from the substrate to the adatoms is mainly due to the surface platinum atoms, which causes a further decrease in the OP. The OP of the Pt$_{(1)}$−Pt$_{(2)}$ bond is similar to that of the corresponding bare slab, whereas the OP for the Pt$_{(2)}$−Pt$_{(2)}$ bond is 0.119 electrons and is similar to the OP obtained from the platinum bulk calculation (0.117 electrons). That the O/S3$_{fcc}$ and O/S4$_{fcc}$ give practically the same binding energies is not surprising, because their OPs for the O−O and O−Pt$_{(1)}$ bonds are practically equal. The O/S2$_{fcc}$ system gives a more negative value for the OP of the O−O bond and a lower value for the OP of the O−Pt$_{(1)}$ bond. These features are an indication of increased repulsive attraction between the oxygen adatoms and a weaker O−Pt$_{(1)}$ bond and can explain the lower binding energy for the O/S2$_{fcc}$ system.

Electronic structure can be further examined by means of density of states (DOS) analysis. In Figure 5 the projected density of states (PDOS) of the individual atoms for the O/S4$_{fcc}$ system is presented for an energy range from −13 to 5 eV, where Fermi energy is set as zero level. Corresponding integrated density of states (IDOS) curves are plotted as well. The comparison of the DOS and PDOSs curves in Figure 5 reveals two prominent peaks at 7 and 9 eV below Fermi energy

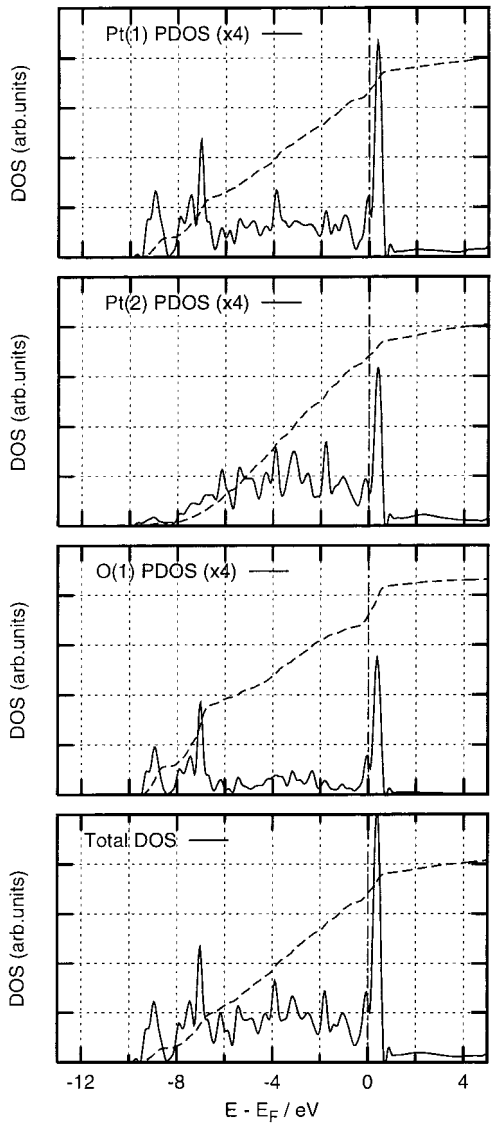


**Figure 5.** LDA/VWN density of states for the $O/S4_{fcc}$ system at equilibrium adsorbate-surface distance projected to its constituent atoms (PDOS) and total density of states (DOS). PDOSs are magnified four times ($\times 4$) with respect to total DOS. Integrated densities of states are drawn as well (dashed line). From top to bottom: PDOSs of $Pt_{(1)}$, $Pt_{(2)}$, $O_{(1)}$, and the total DOS. Note the two oxygen derived prominent peaks at 7 and 9 eV below the Fermi energy.

which appeared after the oxygen adsorption. These oxygen induced structures of the DOS are characteristic of the oxygen adsorption on all transition metals and always appear about 7 eV below the Fermi energy.[53] A further investigation of the DOS features is presented in Figure 6, where the DOS is projected to the 6s and 5d orbitals of the surface platinum atom and to the 2p orbitals of the oxygen adatom. The oxygen-derived structure is mainly due to the $2p_x$ and $2p_y$ oxygen orbitals and to a minor extent due to the $2p_z$ orbital. The most involved orbitals of the platinum surface atom in the adsorbate/surface bond are $5d_{xz}$ and $5d_{yz}$. Also, the contribution of the 6s, $5d_{x^2-y^2}$ and $5d_{xy}$ orbitals in the adsorbate/surface bond is mentionable. We should stress that the above DOS analysis is subjected to large set of bands (27 valence and 4 virtual bands for the discussed energy range); thus, the answer about the energy localization of the different chemical contributions cannot be affected by DOS computational errors as discussed in refs 54−56. The analysis of the crystalline orbital composition in the different energy ranges is a kind of Mulliken analysis of the electronic structure projected onto energy space; thus, all previously specified caution about Mulliken population analysis apply.

An interesting feature of this study is the insensitivity of the binding energy to the number of Pt layers. The $p(1\times1)$ overlayer seems to have less of a perturbing effect to the underneath Pt layers than a $p(2\times2)$ overlayer, since the $p(1\times1)$ overlayer prevents lateral displacement of the surface Pt atoms due to symmetrical constraints. Electron difference density plots on Figure 7 reveal practically the same bonding picture of O−Pt bonds for all three slabs. This picture is also confirmed by Mulliken overlap population analysis (Table 5).

Feibelman has shown that the $p(2\times2)$ fcc-hcp binding energy difference results from d-electron depletion between the first- and second-neighbor Pt atoms in the fcc binding geometry, which does not occur in the hcp case.[27] Thus, it remains to verify such changes in local density distribution. Following Feibelman, the O atom binds relatively weakly in an hcp site, because the d electrons on its Pt neighbors are "frustrated" by two incompatible demands: to move far away from the negatively charged O atoms and to avoid weakening the Pt−Pt bonds by filling the antibonding d states. The difference between $p(2\times2)$ and $p(1\times1)$ adsorption structures is two kinds of subsurface atoms in the former case, whereas all subsurface atoms are equivalent in the latter. Thus, it is sufficient to examine the local density distribution shown in Figure 7 for the $p(1\times1)$ adsorption structure. From this figure it is seen that oxygen is negatively charged (large bright ball). The $d_\sigma$ orbital of the surface Pt atom is clearly seen as two black dots lying along the O−Pt axis. This orbital lacks of electron charge, which minimizes the electrostatic interaction with the adjacent O adatom. Other d orbitals ($d_\pi$, $d_\delta$) possess an excess charge (bright clover-like shape). Since Fermi energy lies near the top of the d bands (Figure 6), adding a high lying d electron would weaken the bond, while removing it would strengthen the bond. In the fcc case, the less electron occupied $d_\sigma$ orbital is oriented toward the subsurface Pt atoms (strengthening of the bond), whereas in the hcp situation, the more electron occupied orbitals are oriented toward the subsurface Pt atom (weakening of the bond).

The two-layer slab model does not posses a subsurface layer. The absent interaction of the surface layer with subsurface layer is a probable reason for difference of about 0.2 eV in oxygen binding energy between the S2 slab with respect to the S3 or the S4 slab. Nevertheless, to explain the preference of fcc vs hcp binding site for S2, the same arguments about d-electron "frustration" might be used; namely, for the fcc case the less electron occupied $d_\sigma$ orbitals of the opposite surface Pt atoms are oriented toward each other, whereas for the hcp case the more electron occupied orbitals are oriented towards each other (see Figure 7).

Finally, a probable explanation of the similarity between the interaction potentials for different spin states will be outlined. At adsorbate−surface distances around 1.3 Å, all three investigated spin states give similar interaction potentials especially in the singlet and triplet states, whereas the interaction potentials for the triplet and pentet states are similar throughout, particularly in the region between 1.7 and 4.0 Å, as shown in Figure 3. To explain this feature, Mulliken population analysis and 3D spin density plots were applied. The Mulliken population analysis at the adsorbate−surface distance of 1.3 Å reveals that all spin states give a net charge transfer of about 0.3 electrons from the substrate to adatom. For all spin states the same atomic orbitals are involved in the adsorbate/substrate bond. These orbitals are also spin populated for the triplet and pentet state,

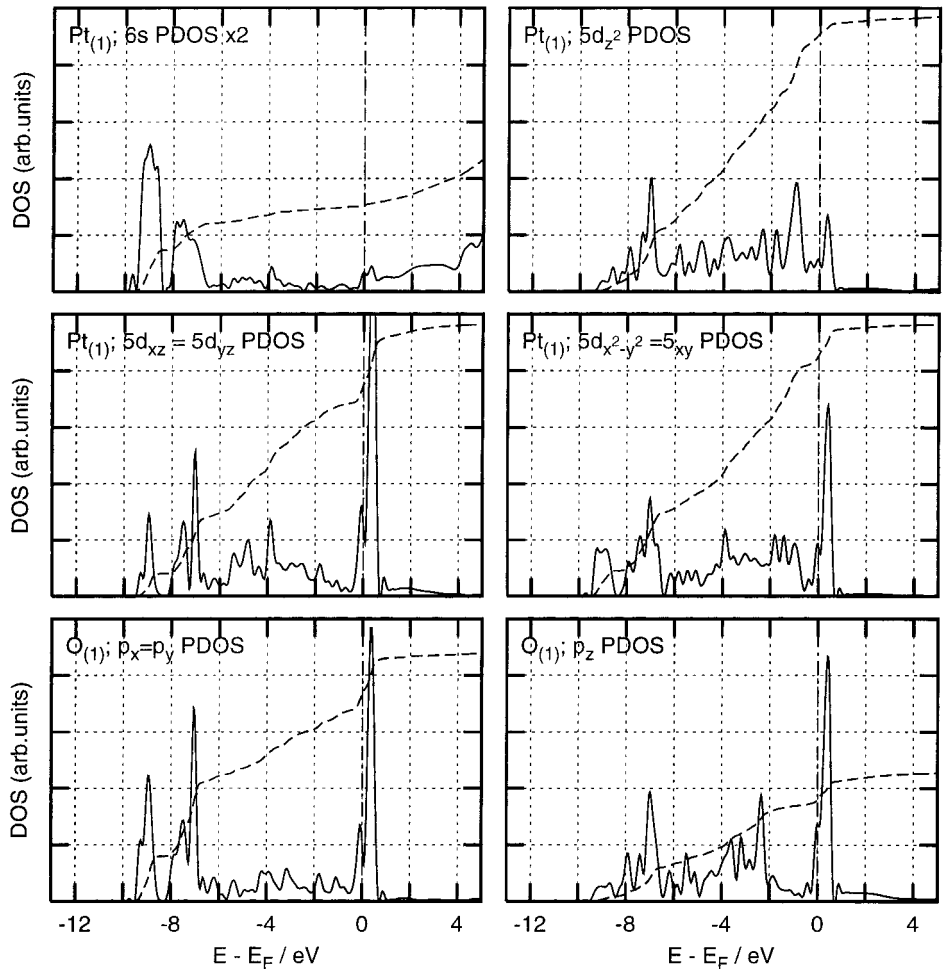


**Figure 6.** LDA/VWN projected density of states (PDOS) analysis of 6s and 5d orbitals of $Pt_{(1)}$ atom and 2p orbitals of $O_{(1)}$ atom for $O/S4_{fcc}$ system at equilibrium adsorbate-surface distance. PDOS of 6s orbital of $Pt_{(1)}$ atom is magnified twice (×2). Integrated density of states is drawn as well (dashed line). Top left: PDOS of 6s orbital for $Pt_{(1)}$ atom; top right: PDOS of $5d_{z^2}$ orbital for $Pt_{(1)}$ atom. Middle left: PDOS of $5d_{xz}$ and/or $5d_{yz}$ orbital for $Pt_{(1)}$ atom. Middle right: PDOS of $5d_{xy}$ and/or $5d_{x^2-y^2}$ orbital for $Pt_{(1)}$ atom. Bottom left: PDOS of $2p_x$ and/or $2p_y$ orbital for $O_{(1)}$ atom. Bottom right: PDOS of $2p_z$ orbital for the $O_{(1)}$ atom.

**TABLE 6: Comparison of the Overlap Population (OP) of Different Spin Multiplicity for $O/S4_{fcc}$ System near Equilibrium Adsorbate−Surface Distance (1.3 Å for Singlet and Triplet Multiplicities and 1.4 Å for Pentet Multiplicity)[a]**

| | singlet | triplet | pentet |
|---|---|---|---|
| bond | total (spin) | total (spin) | total (spin) |
| O−O | −0.003 (0.000) | −0.004 (−0.002) | −0.005 (−0.004) |
| $O-Pt_{(1)}$ | 0.080 (0.000) | 0.077 (−0.032) | 0.073 (−0.058) |
| $Pt_{(1)}-Pt_{(1)}$ | 0.060 (0.000) | 0.062 (−0.001) | 0.074 (−0.005) |
| $Pt_{(2)}-Pt_{(2)}$ | 0.119 (0.000) | 0.120 (−0.009) | 0.120 (−0.012) |

[a] OPs obtained by using spin density matrix are reported in parentheses.

thus the argument that spin is not involved in the bonding seems to be invalid. OPs for some bonds obtained from total and spin density matrices are reported in Table 6. The OP of the $O-Pt_{(1)}$ bond is reduced when going from the singlet to the pentet state, whereas its spin OP is quite negative for triplet and pentet states. All other spin OPs are very small. There is also an increase of the OPs for the $Pt_{(1)} - Pt_{(1)}$ bond when going from the singlet to the pentet state. In Figure 8 the 3D electron spin density of the $O/S4_{fcc}$ is shown. The isosurface of 0.016 and 0.032 au is drawn for the triplet and pentet state, respectively. The isovalue for the pentet state is two times larger, because the pentet state possesses two times more spin than the triplet state does. The main characteristic of the spin density for the triplet state is its symmetry. The surface layer is located in a heterogeneous environment, because it is sandwiched between the oxygen and platinum layer; yet, the spin density is symmetric, indicating that spin is not directly involved in the chemical bonding. This cannot be recognized from the spin population analysis. The spin density for the pentet state is symmetric as well, but the subsurface spin clouds are more egg-like. Again symmetric spin density indicates an indirect participation of the spin in the chemical bonding, therefore the interaction potential of the pentet state is still similar to the singlet one.

When the oxygen monolayer dissociates from the platinum surface, the O/S*X* systems with different spin multiplicities should dissociate into fragments possessing different spin. Most likely, the dissociation limits should be

$$O/SX(0) \rightarrow 2O_{ML}(0) + SX(0)$$

$$O/SX(2) \rightarrow 2O_{ML}(2) + SX(-2)$$

$$O/SX(4) \rightarrow 2O_{ML}(2) + SX(0)$$

where the numbers in parentheses represent the difference of alpha and beta electrons, i.e., $N(\alpha)-N(\beta)$. According to the above processes the dissociation limits for singlet and pentet states should be 2.28 and 0.00 eV above zero energy, respectively, whereas dissociation limits for the triplet state should be 1.16, 1.02, and 0.95 eV above zero energy for O/S2, O/S3,

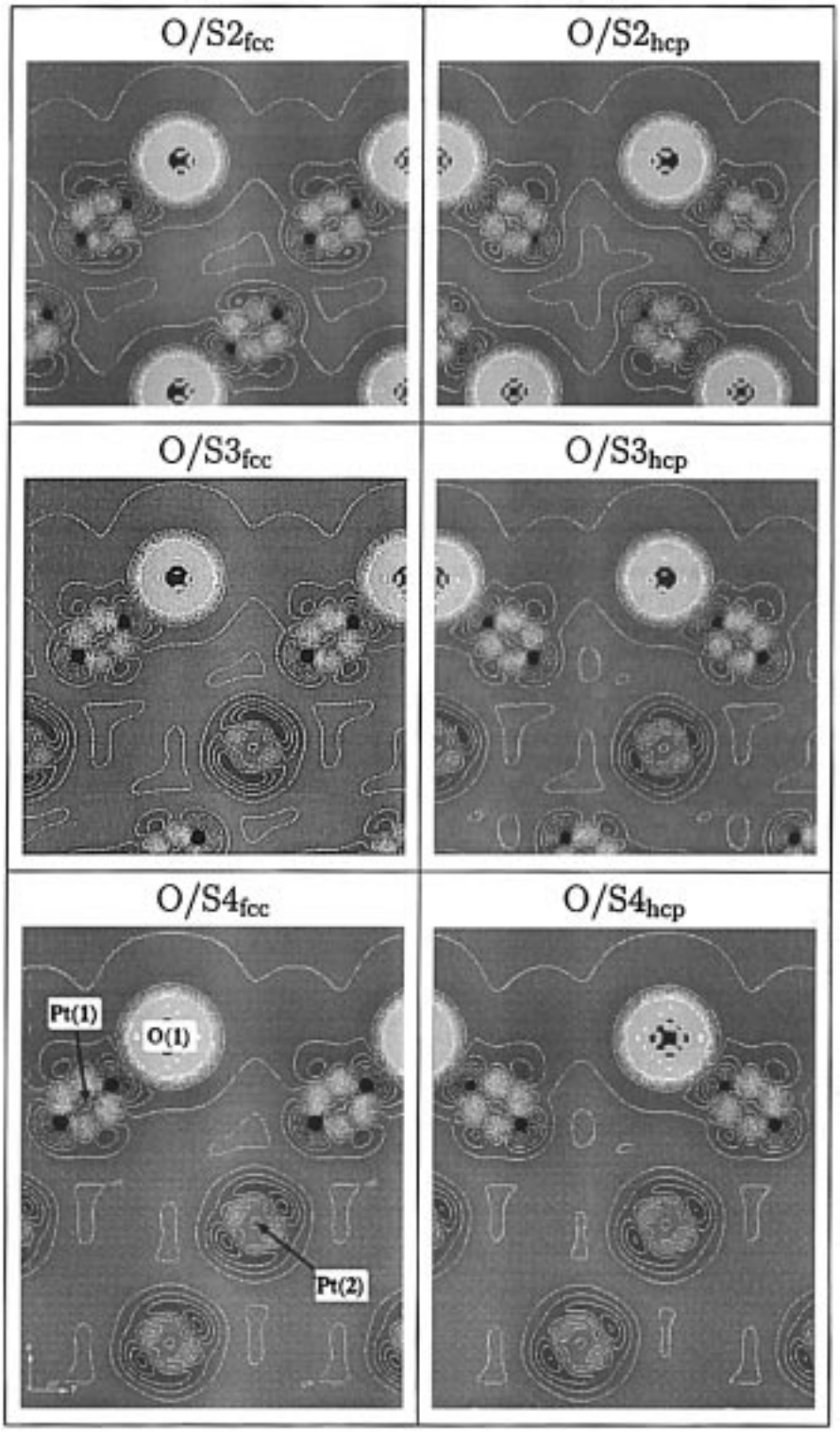


**Figure 7.** LDA/VWN difference electron densities in a $(1\bar{1}0)$ plane for fcc and hcp O/S$X$ ($X$ = 2, 3, and 4) systems at equilibrium adsorbate−surface distances. Difference electron densities were obtained by subtracting O/S$X$ densities from a superposition of individual atomic densities, i.e., $\rho(\mathrm{O/S}X) - [\rho(\mathrm{Pt_{atoms}}) + \rho(\mathrm{O_{atoms}})]$. Dark color represents less electron occupied regions, whereas bright color represents more electron occupied regions. The contours are between −0.07 and 0.07 au with increments of 0.01 au. Some small dots near the oxygen nucleus are artifacts of the interpolation. (These pictures were produced with the *XCrySDen* graphical package.[52])

and O/S4 systems, respectively. Thus singlet and pentet states of the system give expected dissociation limits for oxygen monolayer dissociating from the platinum surface, as evident from Figure 3, while the triplet state does not. At the adsorbate-surface distances of 5.0 Å the spin charge for the $\mathrm{O/S3_{fcc}}$ is −1.60 and 1.80 au for the S3 slab per cell and oxygen adatom (note that there is one oxygen monolayer adsorbed on each side of the slab, i.e., $-1.60 + 2 \times 1.80 = 2.00$), respectively.

## Conclusions

Chemisorption of the atomic oxygen on the Pt(111) surface has been studied by means of the periodic density functional

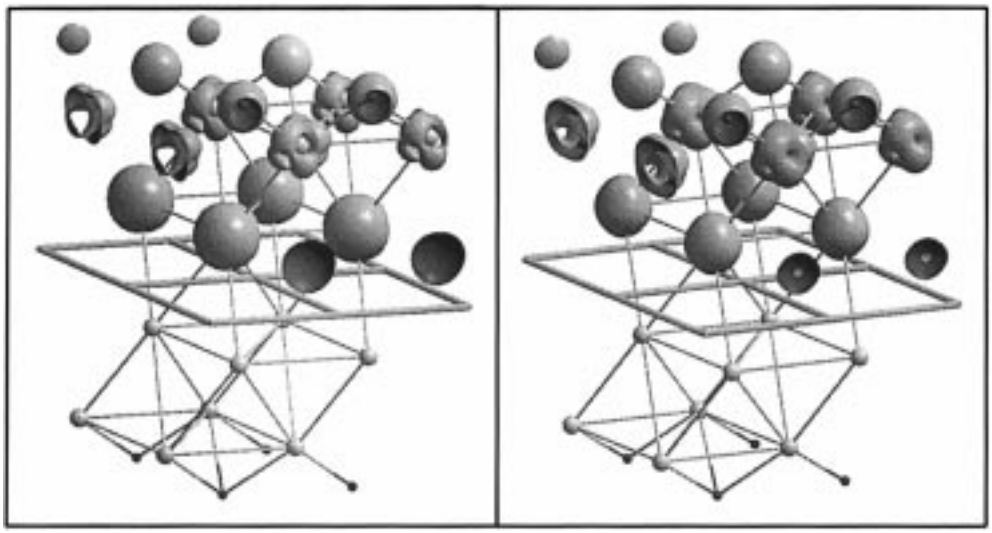

**Figure 8.** LDA/VWN spin electron density of the $O/S4_{fcc}$ system at the equilibrium adsorbate−surface distance. Left: isosurface of 0.016 au for triplet spin multiplicity. Right: isosurface of 0.032 au for pentet spin multiplicity. Two unit cells in both crystallographic directions parallel to the (111) surface are drawn as indicated by unit cell borders in the middle of slabs. The spin electron densities are cut along the outborders. Note that spin densities are very symmetric. (These pictures were produced with the *XCrySDen* graphical package.[52])

approach. The surface was described by two-, three- and, four-layer slabs. Oxygen adatoms were adsorbed on both sides of the slabs in the p(1×1) periodicity. The relaxation and reconstruction of the surface were not taken into account in the present calculations, since we showed that the relaxation of the surface layer is negligible for surface energetics, and reconstruction is not likely to occur in p(1×1) adsorption due to the symmetry restrictions. Some of the important results are as follows.

(**i**) This study underlines a rather good convergence of binding energies $E_b$ with respect to the increasing slab thickness. Binding energies of the singlet state obtained for the three-layer slab are practically the same as those for the four-layer slab, whereas binding energies obtained for the two-layer slab are 0.22 and 0.19 eV lower for the fcc- and hcp-hollow site oxygen positions, respectively.

(**ii**) The oxygen atom prefers to adsorb on the fcc-hollow site and the singlet state was found to be the most stable, the difference being 0.29 eV. The corresponding heats of adsorption obtained from three- and four-layer slab calculations are 1.85 and 0.61 eV for LDA/VWN and BPW91 methods, respectively, whereas the calculated equilibrium adsorbate−surface distances are 1.265 and 1.25 Å for LDA/VWN and BPW91, respectively. The origin of fcc vs hcp binding preference for p(1×1) adsorption structure is the d-electron depletion between the surface and the subsurface Pt atoms in the fcc binding geometry, which does not occur in the hcp case, and is essentially the same as that for the p(2×2) case.[27]

(**iii**) Mulliken population analysis indicates that a net charge of ∼0.3 electrons is transferred from substrate to oxygen adatom. The charge transfer originates from the $5d_{xz}$, $5d_{yz}$, and 6s atomic orbitals of the surface platinum atom and is compensated by the $2p_x$ and $2p_y$ orbitals of the oxygen adatom.

(**iv**) Density-of-states (DOS) analysis reveals two oxygen-derived prominent peaks at 7 and 9 eV below Fermi energy. Further DOS analysis confirms that the $5d_{xz}$ and $5d_{yz}$ orbitals of the surface platinum atom and the $2p_x$ and $2p_y$ orbitals of the oxygen adatom mainly participate in the adsorbate/surface chemical bond. Also a moderate participation of the $5d_{x^2-y^2}$, $5d_{xy}$, and 6s orbitals of the surface platinum orbitals should be mentioned.

(**v**) 3D difference electron density plots show that the oxygen electron cloud is spherical, indicating a delocalized interaction of the oxygen adatom with the surface. The delocalization is consistent with the metal character of the O/SX (X = 2, 3, and 4) systems.

(**vi**) Similarity of binding energies for different spin states is explained in terms of the symmetric spin densities for the triplet and pentet states indicating that the spin is not directly involved in the chemical bonding.

The calculated heat of adsorption seems to rapidly converge with respect to slab thickness. A slab composed of three layers is a very good compromise between the accuracy of the model and the computation time. Even a two-layer slab should yield a moderate description of the adsorption phenomena, since it gives only a 6% lower binding energy and about a 3% larger equilibrium adsorbate−surface distance than three- and four-layer slabs.

Finally, it is noted that the slab model predicts the equilibrium adsorbate−surface distance in reasonable agreement with the experimental data. Calculations performed at the LDA/VWN level overestimate the heat of adsorption, whereas the BPW91 calculated heat of adsorption of 0.61 eV lies between experimental data of Yeo et al.[14] and Parker et al.[15] The extrapolation of the former data gives the adsorption heat of about 1.15 eV at full coverage ($\theta = 1$), but the latter estimated the heat of adsorption to be less than 0.5 eV for the coverages ≥0.75 ML.

**Acknowledgment.** Financial support of this work was provided by the Ministry of Science and Technology of Slovenia, Grant J1-7339. The authors thank I. Kobal, P. W. M. Jacobs, Y. F. Zhuhovskii, and U. Borštnik for reading the manuscript and helpful discussions.

## References and Notes

(1) Engel, T.; Ertl, G. *Adv. Catal.* **1979**, *28*, 1.
(2) Engel, T.; Ertl, G. Oxidation of Carbon Monoxide. In *The Chemical Physics of Solids Surfaces and Heterogeneous Catalysis*; King, D. W., Woodruff, D. P., Eds.; Elsevier Scientific Publishing Company: Amsterdam, 1982; Vol. 4, pp. 73−93.
(3) Matsushima, T. *Heterog. Chem. Rev.* **1995**, *2*, 51.
(4) Reutt-Robey, J. E.; Doren, D. J.; Chabal, Y. J.; Christman, S. B. *Phys. Rev. Lett.* **1988**, *63*, 2778.
(5) Gland, J. L. *Surf. Sci.* **1980**, *93*, 487.
(6) Campbell, C. T.; Ertl, G.; Kuipers, H.; Segner, J. *J. Chem. Phys.* **1980**, *73*, 5863.
(7) Gland, J. L.; Sexton, B. A.; Fisher, G. B. *Surf. Sci.* **1980**, *95*, 587.

(8) Campbell, C. T.; Ertl, G.; Kuipers, H.; Segner, J. *Surf. Sci.* **1981**, *107*, 221.
(9) Luntz, A. C.; Williams, M. D.; Bethune, D. S. *J. Chem. Phys.* **1988**, *89*, 4381.
(10) Mortensen, K.; Klink, C.; Jensen, F.; Besenbacher, F.; Stensgaard, I. *Surf. Sci.* **1989**, *220*, L701.
(11) Puglia, C.; Nilsson, A.; Hernnäs, B.; Karis, O.; Bennich, P.; Martensson, N. *Surf. Sci.* **1995**, *342*, 119.
(12) Starke, U.; Materer, N.; Barbieri, A.; Döll, R.; Heinz, K.; Van Hove, M. A.; Somorjai, G. A. *Surf. Sci.* **1993**, *287/288*, 432.
(13) Materer, N.; Starke, U.; Barbieri, A.; Döll, R.; Heinz, K.; Van Hove, M. A.; Somorjai, G. A. *Surf. Sci.* **1995**, *325*, 207.
(14) Yeo, Y. Y.; Vattuone, L.; King, D. A. *J. Chem. Phys.* **1997**, *106*, 392.
(15) Parker, D. H.; Bartram, M. H.; Koel, B. E. *Surf. Sci.* **1989**, *217*, 489.
(16) Steininger, H.; Lehwald, S.; Ibach, H. *Surf. Sci.* **1982**, *123*, 1.
(17) Derry, G. N.; Ross, P. N. *Surf. Sci.* **1984**, *140*, 165.
(18) Neuhaus, D.; Joo, F.; Feuerbacher, B. *Phys. Rew. Lett.* **1987**, *58*, 694.
(19) El-Issa, B. D.; Hinchliffe, A. *Mol. Phys.* **1980**, *39*, 1463.
(20) Ray, N. K.; Anderson, A. B. *Surf. Sci.* **1982**, *119*, 35.
(21) Zhou, R. H.; Cao, P. L. *Phys. Lett. A* **1992**, *169*, 167.
(22) Illas, F.; Rubio, J.; Ricart, J. M.; Pacchioni, G. *J. Chem. Phys.* **1996**, *105*, 7192.
(23) Kokalj, A.; Lesar, A.; Hodošček, M. *Chem. Phys. Lett.* **1997**, *268*, 43.
(24) Chan, A. W. E.; Hoffmann, R.; Ho, W. *Langmuir* **1992**, *8*, 1111.
(25) Feibelman, P. J.; Esch, S.; Michely, T. *Phys. Rev. Lett.* **1996**, *77*, 2257.
(26) Feibelman, P. J. *Phys. Rev. B* **1997**, *56*, 2175.
(27) Feibelman, P. J. *Phys. Rev. B* **1997**, *56*, 10532.
(28) Eichler, A.; Hafner, J. *Phys. Rev. Lett.* **1997**, *79*, 4481.
(29) Bogicevic, A.; Strömquist, J.; Lundqvist, B. I. *Phys. Rev. B* **1997**, *57*, R4289.
(30) Alavi, A.; Hu, P.; Deutsch, T.; Silvestrelli, P. L.; Hutter, J. *Phys. Rev. Lett.* **1998**, *80*, 3650.
(31) Feibelman, P. J.; Hafner, J.; Kresse, G. *Phys. Rev. B* **1998**, *58*, 2179.
(32) Kokalj A.; Causà, M. *J. Phys. Condens. Matter*. Submitted for publication.
(33) Dovesi, R.; Saunders, V. R.; Roetti, C.; Causá, M.; Harrison, N. M.; Orlando, R.; Aprá, E. *CRYSTAL95 User's Manual*; University of Torino: Torino, Italy, 1996.
(34) Stevens, W. J.; Krauss, M.; Bash, H.; Jansien, P. G. *Can. J. Chem.* **1992**, *70*, 612.
(35) The results using RECP of Stevens et al.[34] without f-projection term were not published but were performed in conjunction with our previous cluster study, ref 23.
(36) McLean, A. D.; Chandler, G. S. *J. Chem. Phys.* **1980**, *72*, 5639. Krishnan, R.; Binkley, J. S.; Seeger, R.; People, J. A. *J. Chem. Phys.* **1980**, *72*, 650.
(37) Dirac, P. A. M. *Proc. Cambridge Phil. Soc.* **1930**, *26*, 376.
(38) Vosko, S. H.; Wilk, L.; Nusair, M. *Can. J. Phys.* **1980**, *58*, 1200.
(39) Becke, A. D. *Phys. Rev. A* **1988**, *38*, 376.
(40) Perdew, J. P.; Wang, Y. *Phys. Rev. B* **1986**, *33*, 8800. **1989**, *40*, 3399; *Phys. Rev.* **1992**, *45*, 13244.
(41) Dovesi, R.; Pisani, C.; Ricca, F.; Roetti, C. *Phys. Rev. B* **1982**, *25*, 3731.
(42) Dovesi, R.; Ferrero, E.; Pisani, C.; Roetti, C. *Z. Phys. B* **1983**, *51*, 195.
(43) Dovesi, R.; Pisani, C.; Roetti, C. *Gazz. Chim. Ital.* **1983**, *113*, 313.
(44) Feibelman, P. J. *Phys. Rev. B* **1995**, *51*, 17687.
(45) Moruzzi, V. L.; Janak, J. F.; Williams, A. R. *Calculated Electronic Properties of Metals*; Pergamon Press, New York, 1978; pp. 11−14.
(46) Pulay, P. *Chem. Phys. Lett.* **1980**, *73*, 393.
(47) Monkhorst, H. J.; Pack, J. D. *Phys. Rev. B* **1976**, *13*, 5188.
(48) Gilat G.; Raubenheimer, L. J. *Phys. Rev.* **1966**, *144*, 390. Gilat, G. *J. Comp. Phys.* **1972**, *10*, 432.
(49) Wyckoff, R. W. G. *Crystal Structures*, 2nd ed.; Interscience: New York, 1963.
(50) Ge, Q.; Hu, P.; King, D. A.; Lee, M. H.; White, J. A.; Payne, M. C. *J. Chem. Phys.* **1997**, *106*, 1210.
(51) Wright, J. S.; Shih, S. *Chem. Phys. Lett.* **1976**, *42*, 383. Krishna, M. V. R.; Jordan, K. D. *Chem. Phys.* **1987**, *115*, 423.
(52) All high-quality three dimensional plots in this paper are produced by XCrySDen graphical package, which was developed during the past three years by the following authors: Kokalj, A. *J. Mol. Graphics Model.* Submitted for publication. Kokalj, A.; Causa, M. To be submitted.
(53) Varma, C. M.; Wilson, A. J. *Phys. Rev. B* **1980**, *22*, 3795. Wilson, A. J.; Varma, C. M. *J. Phys. Rev. B* **1980**, *22*, 3805.
(54) Pisani, C.; Aprà, E.; Causà, M. *Int. J. Quantum Chem.* **1990**, *38*, 395.
(55) Pisani, C.; Aprà, E.; Causà, M.; Orlando, R. *Int. J. Quantum Chem.* **1990**, *38*, 395.
(56) Pisani, C.; Dovesi, R.; Roetti, C. *Hartree-Fock Ab Initio Treatment of Crystalline Systems*; Springer-Verlag: Heidelberg, 1988.